Applications of Ultrafast Lasers to Two-Photon Fluorescence and Lifetime Imaging

N.P.Barry[a•], K.M.Hanson[a], E.Gratton[a], R.M.Clegg[a], M.J.Behne[b], T.M.Mauro[b]
[a]Laboratory for Fluorescence Dynamics, University of Illinois at Urbana Champaign.
[b]Dept. of Dermatology, UCSF & VAMC Dermatology Service, San Francisco, CA

ABSTRACT

Fluorescent probes have found widespread use in biomedical sciences. Particularly since they can be targeted to cellular compartments and further more can report on the properties of their environment such as calcium concentration.

Near infrared ultrafast lasers find increasing use for fluorescence applications since femtosecond pulses with a few milliwatts of average power are sufficient to induce significant two photon fluorescence from the probe when focussed into typical samples. The nonlinear optical excitation process allows sectioned imaging of 3-D samples without use of a confocal pinhole. In this paper we describe two aspects of multiphoton microscopy: the two-photon excitation cross section and the fluorescence lifetime.

Of interest is the wavelength characterization of two-photon excitation cross-sections of fluorescence probes. We slowly modulate (~500Hz) the intensity envelope of the input laser pulse train and analyze the emission signal in terms of the amplitude and phase of the harmonics of this modulation. In effect this is a power study that allows separation of different order effects.

An application of ultrafast laser excitation that exploits many of the features outlined above is measurement of pH gradients in the skin. This is essential to skin barrier function and disruption of the gradient is though to be a indicating factor in many skin diseases. A probe for which the fluorescence lifetime varies with pH is used. We thus are able to tackle problems associated with inhomogeneous labeling. We have developed a two-photon laser-scanning lifetime microscope and present pH maps of skin obtained with this instrument.

Keywords

Two-photon excitation, microscopy, cross-section, fluorescence lifetime imaging, functional imaging. Skin.

1. INTRODUCTION

Ultrafast lasers are finding ever increasing use in the fields of biomedical and biophysical sciences. Commercialization of modelocked lasers has resulted in robust, stable and broadly tunable sources suitable for use in non-specialist laser laboratories. Techniques have been demonstrated that exploit either the very short time duration of ultrafast pulses (e.g femtosecond reaction kinetics) or the non-linear optical response induced by the high peak powers of typical ultrafast laser pulses. Much of the development of non-linear optical techniques in biomedical and biophysical sciences can be correlated to the introduction of the picosecond and femtosecond pulsed Titanium Sapphire laser. For two-photon excitation fluorescence, its wavelength tuning range from 700nm to 1000 nm provides a good match to the excitation energies of fluorescent labels that were originally developed with single photon UV/ visible excitation in mind. Practical experience has shown that other types of short-pulse laser such as modelocked Nd:YAG and and Nd:Glass lasers can offer advantages over the Ti:Sapphire laser in certain applications, typically a consequence of the differing wavelength range that they offer access to.

In this paper we discuss the application of ultrafast lasers to multiphoton excitation fluorescence microscopy[1,2]. We focus on two techniques:- the measurement of the two-photon excitation cross-section and the use of fluorescence lifetime to yield functional information.

Multi-photon microscopy represents the most widespread application of ultrafast lasers in the biomedical sciences, though a diversity of other techniques are constantly increasing in prevalence. The key advantage of this application is that nonlinear optical excitation allows sectioned imaging of 3-D samples without use of a confocal pinhole. This can significantly simplify instrument design. Optical resolution comparable to commercial confocal

• Corresponding author: N.P.Barry www.lfd@uiuc.edu tel 217 244 5620

Commercial and Biomedical Applications of Ultrafast and Free-Electron Lasers,
Glenn S. Edwards, Joseph Neev, Andreas Ostendorf, John C. Sutherland, Editors,
Proceedings of SPIE Vol. 4633 (2002) © 2002 SPIE · 0277-786X/02/$15.00

microscopes is achievable with a few milliWatts of average power at the sample. Further advantages of NIR excitation are the increased penetration depth into scattering samples compared to one photon excitation of fluorophores and the large spectral separation between excitation and emission wavelengths. [2,3,4]

There exist a multitude of Fluorescent probes, developed for labeling of bio-molecules and cell compartments. These probes can report on a variety of chemical environments such as calcium concentration and pH, or be targeted to particular molecules e.g. nuclear stains and membrane stains. There is much interest in characterizing the two photon excitation spectra of these dyes such that they may be used under optimum conditions in two-photon microscopy.

2. TWO PHOTON CROSS SECTION MEASUREMENT

Whilst the emission spectrum of a fluorophore is generally not different under multiphoton excitation compared to single photon excitation, there are questions of photostability or existence of higher order excitation processes (three photon excitation). We address both these issues by slowly modulating (100 to 1000 Hz) the intensity envelope of the input laser pulse train. This may be viewed in two ways: - our measurement is intrinsically a power study of the excitation process. This enables the distinction between scatter, two-photon and three-photon processes. Secondly, modulating the excitation light can give information regarding the time dynamics of the fluorescence signal. Time information is derived from the phase of the harmonic content of the emitted light compared to the excitation signal. This additional dimension to our data can in principle help to distinguish between a 'fast' process e.g. presence of a three-photon excitation signal and a 'slow' process such as bleaching recovery which is determined by the diffusion of 'fresh' fluorophores into the excitation volume.

The desire for efficient excitation naturally suggests the use of a short pulse laser system (e.g. 100 femtosecond pulse duration) however the chromatic dispersion of the laser pulse in the experimental system may lead to significant uncertainties in the temporal properties of the excitation pulse. It is possible to measure the pulse duration at the sample directly using autocorrelation techniques[5]. Alternatively the use of a picosecond Ti:Sapphire laser, with its smaller spectral bandwidth can reduce this potential source of error to insignificant levels. Many commercial modelocked Ti:Sapphire lasers offer relatively easy conversion between femtosecond and picosecond operation modes. We therefore use picosecond mode for cross section measurement. For subsequent use of a fluorescent probe in a biological sample, where different experimental constraints apply, femtosecond pulsed operation is used. The theoretical description of the multi-photon excitation process has been described extensively in the literature[6-14]. In summary for the case of two-photon absorption, the number of absorbed photons N_{abs} in a sample of concentration C (assumed constant) and sample volume V, when excited by a pulse I(**r**, t) is given by[13]:

$$N_{abs} = \int_V dV \delta C I^2(r,t) \tag{1}$$

Where δ is the two photon absorption cross section. The number of detected photons depends upon the system collection efficiency ϕ, typically wavelength dependent and the fluorescence quantum efficiency η_2 . Assuming no self quenching and stimulated emission, the number of fluorescence photons emitted is:

$$F(t) = \frac{1}{2}\phi\eta_2 N_{abs} \tag{2}$$

The detected fluorescence signal is therefore dependent upon the experimental geometry. In this context, it is convenient to use the diffraction limited spot of a lens as the excitation volume. The typically small (micron) dimensions of this spot favor good two-photon excitation at low average powers from a picosecond or femtosecond pulsed laser. The experimental implementation of this requires that a collimated beam, expanded such that it over fills the aperture of a lens, is focused into a sample volume at a point away from the vessel walls. An experimental convienence is that this lens may also be used to collect the fluorescence signal. The temporal and spatial properties of the excitation pulse may be separated:

$$I(r,t) = I_0(t)S(r) \tag{3}$$

Where S(r) represents the spatial shape of the excitation volume. The volume integral for a diffraction limited spot may be solved numerically noting that for two photon excitation one must integrate over $S(r)^2$.

It is convenient to work in terms of the time averaged fluorescent signal <F(t)> since a slow detector may be used. Similarly it is convenient to measure the average excitation power at the sample <P(t)> rather than intensity $I_0(t)$. For two-photon excitation, <F(t)> is proportional to $<I_0^2(t)>$, hence additional factors , accounting for the temporal pulse

shape g_p, temporal pulse width τ and pulse repetition frequency f, must be introduced to account for the intensity dependent excitation process when working with the average power. Summarising all these factors and integrating over a diffraction limited point spread function yields[13]

$$\langle F(t)\rangle = \frac{1}{2}\phi\eta_2 C\delta\frac{g_2}{f\tau}\frac{8n\langle P(t)\rangle^2}{\pi\lambda} \tag{4}$$

A schematic of the experiment is shown in figure 1.

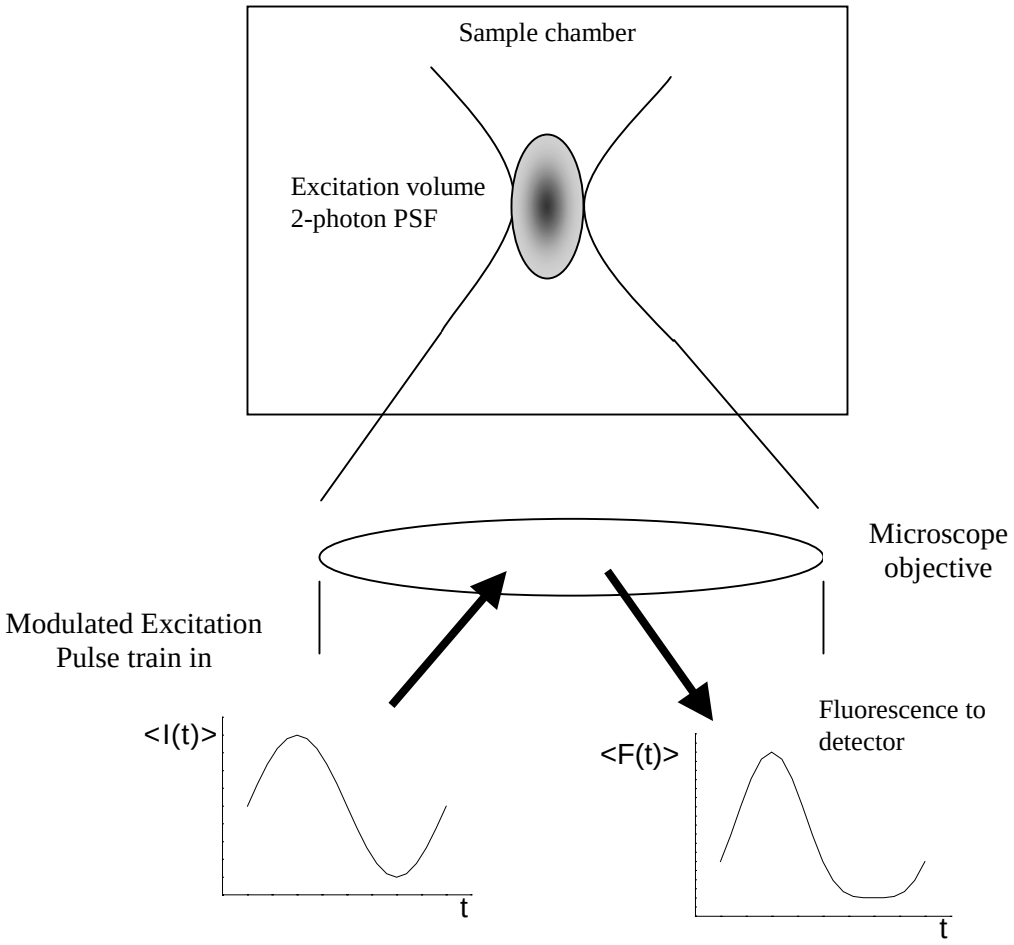

Figure 1: Schematic of two-photon excitation cross-section measurement experiment

In our measurement we slowly modulate the average incident power. Equation (4) remains valid as long as the modulation frequency (10^3 Hz) is much smaller than the pulse repetition frequency (10^8 Hz). The time averaging symbols are retained to indicate that averaging over the pulse to pulse period is still implied. In general, the periodically modulated excitation waveform may be described by a Fourier series and will have a DC offset.

$$\langle P(t)\rangle = DC_{ex}\left(1+\sum\nolimits_i m_{exi}Sin(\omega_i t+\phi_{ex})\right) \tag{5}$$

Similarly the emitted fluorescence can also be described by a Fourier series.

$$\langle F(t)\rangle = DC_f\left(1+\sum\nolimits_i m_{fi}Sin(\omega_i t+\phi_f)\right) \tag{6}$$

In the case of two photon excitation, there is a quadratic relationship between P(t) and F(t).

$$\langle F(t)\rangle = K\left[DC_{ex}\left(1+\sum_i m_{exi} Sin\left(\omega_i t+\phi_{ex}\right)\right)\right]^2 \quad (7)$$

Using the general principles outlined in reaching equation (4) it is possible to include higher order terms e.g. three photon excitation or to include a photobleaching term (exponential decay) in equation (7). The grouped parameter K contains the constants from Equation (4) including the two-photon excitation cross section which may be recovered with suitable instrument calibration.

2.1 Experimental setup

The experimental system consists of an inverted microscope (Zeiss Axiovert 100) and a tunable modelocked Ti:Sapphire laser (Spectra Physics Tsunami). The laser was operated in the picosecond mode giving pulses with a bandwidth of approximately 1 nanometer and a duration close to 1 picosecond. The laser beam was expanded and brought to the sample via the epifluorescence port. The beam was focused into the sample using a Zeiss neofluar 10X 0.3 NA objective. The literature value[15] of group velocity dispersion of 500 fs^2 for this objective indicates that broadening effects may neglected in the picosecond regime.

Modulation of the laser at low frequency (100-1000 Hz) is achieved using an electro-optic modulator driven from a frequency synthesiser. The beam is expanded and then enters the microscope. After expansion a number of components are split off the beam. The wavelength is measured using a wavemeter (IST Rees) and pulse duration measured with an autocorrelator (Femtochrome). A component is also sent to a 'reference' photomultiplier. The fluorescence signal was detected using a 'signal' photomultiplier on the bottom port of the microscope. A suitable combination of microscope dichroic and blocking filter (BG39 Schott glass) was chosen to stop light at the excitation wavelength reaching this detector.

The two photomultiplier signals are simultaneously digitised using a two channel A to D card. The signal was analysed using a commercial software program (ISSL from ISS inc). This program generates an output file containing the digitised signal and reference waveforms, as well as the DC level and harmonic phase and amplitudes of the Fourier components of the signal waveform relative to the reference photomultiplier.

Sample concentrations were determined using manufacturers or published extinction coefficients. Samples were prepared in either hanging drop slides or 8 well slides. Concentrations were adjusted to avoid inner filter effects. A schematic of the experimental apparatus is shown in figure 2.

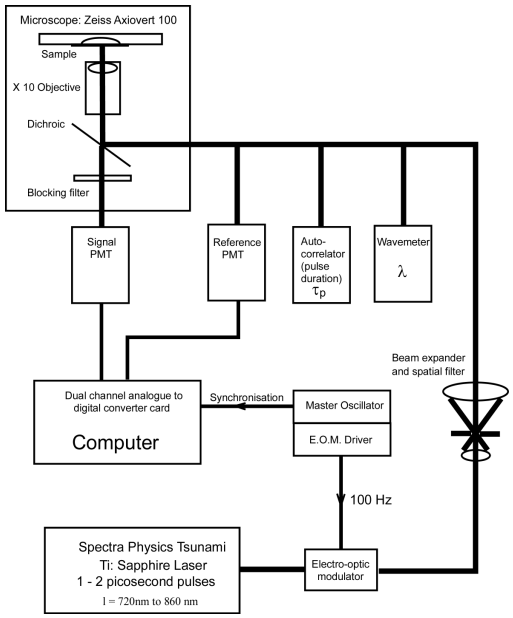

Figure 2: Experimental apparatus used to measure the two-photon excitation cross-section.

2.2 Data analysis.

A typical data set is shown in figure 3. This shows one period of the fluorescence signal from a fluorescein sample. The input excitation pulse train had a sinusoidal envelope with a modulation frequency of 800 Hz. The asymmetric shape of the fluorescence signal is due to the nonlinear excitation process. The squares are the values of the digitized fluorescence signal (a.u.). The solid line is a fit using equation (7). The excitation waveform (equation (5)) used in the fit was calculated from the digitized reference PMT signal.

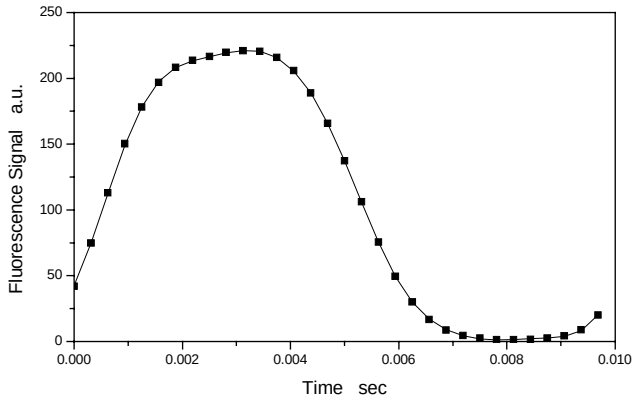

Figure 3:Fluorescence signal from a fluorescein sample (squares) and fit derived from reference PMT signal (solid Line)

The table summarises the measured and fitted data for a number of harmonics of the fluorescence signal.

Frequency (Hz)	Amplitude (au)		Phase (degrees)	
	Experimentally measured fluorescence signal	Calculated values using model and data from reference PMT signal	Experimentally measured fluorescence signal	Calculated values using model and data from the reference PMT signal
0	96.6	96.5		
800	123.1	123.1	-98.7	-99.0
1600	29.1	29.0	-197.6	-198.4
2400	2.2	2.1	-115.9	-118.8
3200	2.0	2.0	-222.3	-221.7
4000	0.2	0.2	-66.8	-339.7

There is good agreement between the measured fluorescence waveform and the fitted waveform, calculated using the reference PMT signal. There is very little amplitude in the third harmonic and higher components suggesting that the excitation process obeys a square law. The agreement between the phase terms suggests, in this instance, that there was no significant photobleaching.

2.3 Calibration

A large number of calibration factors are required in order to measure the two-photon excitation cross-section. Corrections are made for the wavelength sensitivity of the photomultipliers. The emission spectrum of each fluorophore was measured and corrections were made for the wavelength dependent transmission of the microscope dichroic and NIR blocking filter. More difficult to determine are the excitation volume and collection efficiency of the system. The analysis of reference 13 gives a good estimate of the volume, assuming a diffraction limited spot. Pulse durations were

measured at each wavelength using an autocorrelator and a $sech^2$ shape factor of $g_p = 0.588$ was used. This leaves the collection efficiency to be determined. We decided to calibrate our system against published data for fluorescein. A value of $\delta = 38 \pm 9.7 \times 10^{-50}$ cm^4s/photon at 782nm and $\eta_2 = 0.9$ were used. For each experimental run a sample of fluorescein is also measured. Other samples are then measured against this instrument calibration standard. Analysis yields a value for the product of the two-photon quantum efficiency η_2 and the two-photon excitation cross-section δ. Since the value of η_2 is generally not known, we present our data in terms of the product $\eta_2\delta$. Data for a number of fluorophores are shown below in figure 4 a and b the solvents are indicated in brackets.

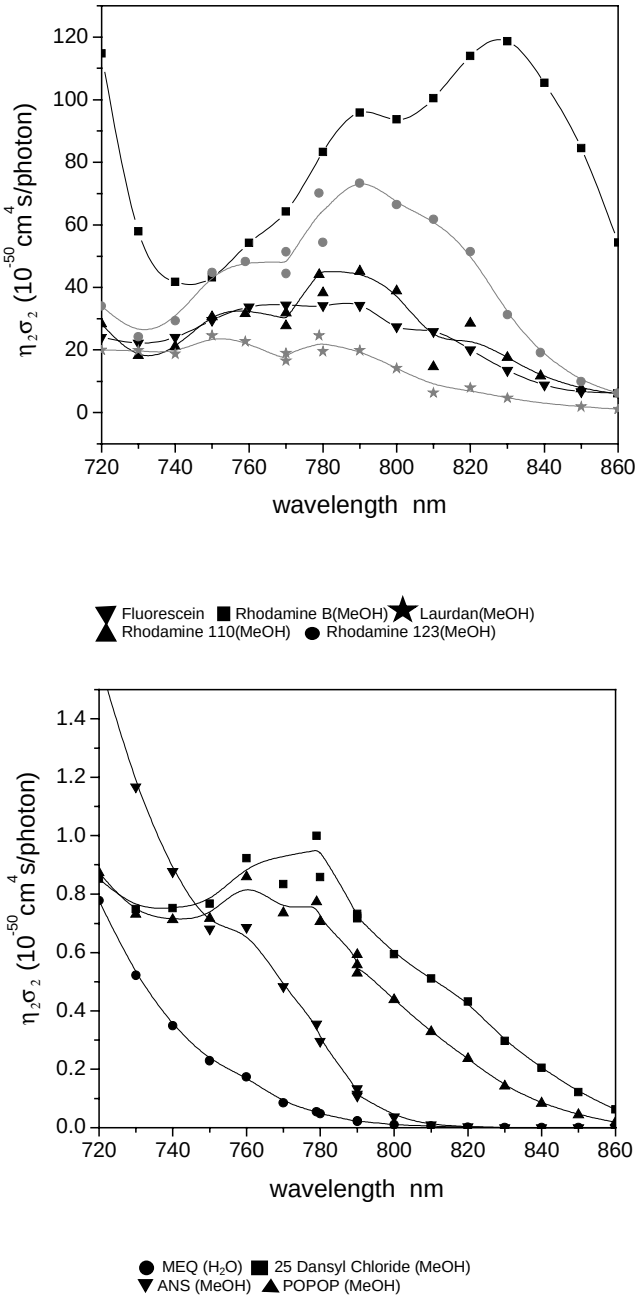

Figure 4a,b: Two-photon excitation cross-section spectra for a number of fluorophores.

3. TWO-PHOTON FLUORESCENCE LIFETIME IMAGING

Fluorescence lifetime imaging offers an additional avenue to obtain quantitative functional information from a sample. In this section we describe our instrument and an example of its use to measure the pH in the stratum corneum of the skin. There are many fluorescent probes that are sensitive to their environment e.g. calcium and pH indicators. The challenge when using these probes in heterogeneous environments is to unambiguously attribute a variation in contrast of the fluorescence signal to the parameter of interest and not merely a local variation in concentration. Typically this problem is addressed using either excitation or emission ratio methods. For full field, lamp based systems these ratiometric methods have been shown to work well.

However the situation becomes more complicated should three dimensional information, with subcellular resolution be required. This is typically the domain of confocal microscopy. In this case the availability of suitable excitation laser lines and the requirement to switch rapidly between them (in the case of excitation ratio method) complicates and may even preclude the use of a particular fluorescent indicator. For many indicators it has been shown that there is also a change in fluorescence lifetime in addition to changes in the excitation/ emission spectrum. This can be due to the fluorophore existing in two forms e.g. a protonated and a deprotonated form in the case of pH , each with its own characteristic fluorescence lifetime[16,17]. It is then possible to measure the required parameter with a single excitation line and single emission channel since the lifetime measurement is not compromised by heterogeneous labeling.

A second consideration is the scattering property of the sample. In the case of thick tissue samples as opposed to monolayers of cultured cells, scattering can rapidly degrade confocal image quality. It has been shown that two-photon excitation can offer increased imaging depth due to the reduced scatter and absorption of NIR light in tissue[3,4]. In addition since there is no pinhole in the detection path, fluorescence photons that are scattered on their path out of the sample can still reach the detector. Whilst scatter will delay the arrival time of a photon and hence increase its apparent lifetime, this effect is insignificant (picoseconds) in microscopy applications compared to the fluorescence lifetime (typically of the order of nanoseconds).

As an example of the power of lifetime based functional imaging, we present data showing the pH distribution in the skin[27]. The outermost layer known as the stratum corneum, forms a barrier that controls water loss and entry, UV absorption and prevents ingress of infectious agents and chemicals. The outer surface is well known to be of lower pH (between 4.5 and 6 depending upon sex, age and location) compared to the normal physiological value of pH 7. It is also known that at the first viable epidermal layer, the stratum granulosum, some 10 to 20 cell layers into the skin this normal pH is found. It is thought that pH plays a vital role in maintenance of the barrier function, however comparatively little is known of the morphology of this 'acid mantle' at a cellular level[18-22]. The standard technique of tape stripping and application of a flat pH electrode[18,19] gives an average measurement over an area of the order of 1 cm^2. In addition the technique disrupts the stratum corneum structure. A method that can map pH with high resolution in the stratum corneum has application to the understanding the physiology of barrier function, skin disease such as dermatitis and the penetration / effect of topically applied drugs and cosmetics.

3.1 Methods

The lifetime imaging instrument is built around a two-photon laser scanning microscope. The primary modification required to the instrument hardware is the addition of lifetime capable detectors. In this application we implemented the heterodyne frequency domain technique to measure fluorescence lifetime. This instrument has been described in the literature[23]. In this method we operate the detection PMTs (Hamamatsu R 928) in the analogue mode. This offers the advantage of higher frame speeds (assuming a bright enough sample), compared to single photon counting techniques. In time correlated single photon counting based systems, the minimum time to acquire an image is limited by pulse pile up in the detector and discriminator reset time.

We used the same instrument (Zeiss Axiovert 100 Microscope and Spectra Physics Tsunami Ti Sapphire Laser) as used to measure excitation cross section. The laser was operated in the femtoseond pulsed mode and was brought into the microscope via a computer controlled X,Y scan mirror (Cambridge Technology) and scan lens such that the laser was focused to a point and a raster scan of the sample was made. A blocking filter (Schott BG39 , Chroma HG 525/50) was used to prevent the excitation light reaching the detector. An oil immersion objective (Zeiss FFluar 40X) was used

to produce a sub micron excitation spot. Z sectioned slices were obtained using a motorized focus driver (ASI Multi scan 4LS).

In the frequency domain technique, the phase and modulation of the fluorescence signal are measured relative to the excitation signal (monitored using a reference PMT). In the case of pulsed excitation, the base excitation frequency is determined by the repetition rate of the laser (80MHz)[24]. The heterodyne detection method, where the high frequency fluorescence signal is mixed with a slightly shifted frequency signal from a reference oscillator to generate a beat frequency at 2.5kHz is used. This low frequency signal, which contains the phase and modulation information required to calculate the fluorescence lifetime can be digitized using a standard analogue to digital converter. In this implementation of the technique, we modulate the PMT at the first dynode with an RF signal. The digitized signals from the sample and reference PMTs were analysed using an FFT algorithm which outputs values of phase and modulation at each pixel of the image. We sample at 8 equally spaced points (50 microseconds each) over a cycle of the beat signal to calculate the lifetime in each pixel. The image is a 256 by 256 pixel array and takes ~30 seconds to acquire. A schematic of the instrument is shown in figure 5.

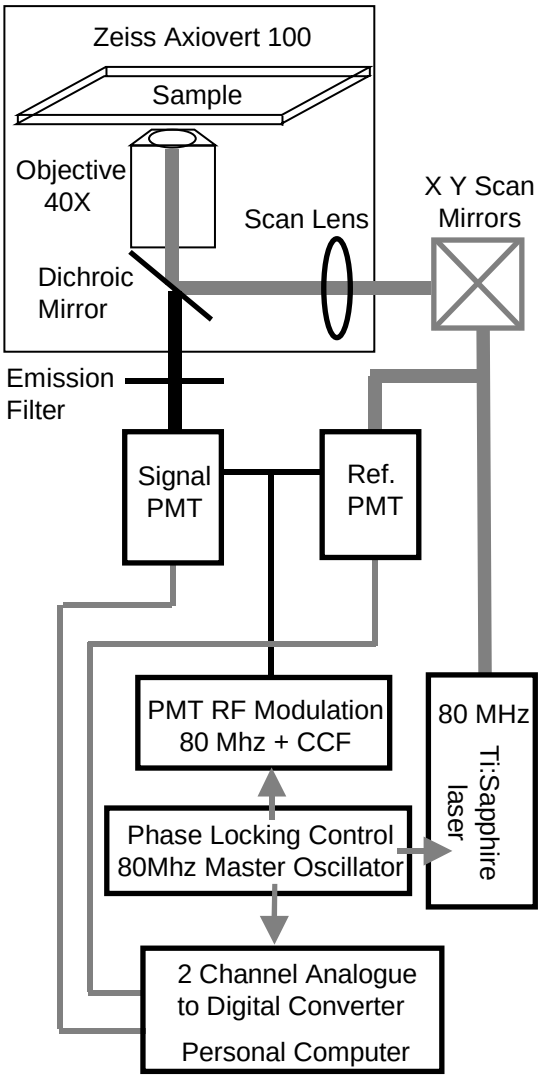

Figure 5: Schematic of two-photon laser scanning fluorescence lifetime microscope.

Skin samples were obtained from hairless mice following protocols approved by the University of Illinois Division of Animal Resources. Skin samples of $1cm^2$ were incubated with 50μL of 50μM BCECF applied to the outer surface for a period of one hour. The autofluorescence intensity was measured using control samples with no dye and was found to be insignificant compared to the signal from the stained samples over the depths of interest.

To probe the pH of the sample we use the dye BCECF (Molecular Probes)[25]. This has a pKa of 7 and has been shown to have a pH dependant lifetime. Calibration measurement in an acidic solution of the dye (pH 4.5) and a basic solution (pH 8.5) yielded lifetimes of 2.75 ± 0.04 n sec and 3.90 ± 0.08 nsec respectively. At pH values in the region of interest, the range from pH 5 to pH 8 the dye exists as a mixture of the protonated and un protonated forms[16]. The measured lifetime will therefore be a weighted average of the two limiting lifetime values, dependent upon their fractional concentration. Assuming the reaction between the two forms can be described as follows:

$$HBCECF \xrightarrow{K_a} H^+ + BCECF^- \tag{8}$$

then the pH is given by the Henderson-Hasselbach equation.

$$pH = pK_a + Log\frac{[BCECF^-]}{[HBCECF]} \tag{9}$$

where $[HBCECF]$ and $[BCECF^-]$ are the concentrations of the protonated and deprotonated forms. This ratio may be deduced from the lifetime measurement. The FFT algorithm yields the phase ϕ and demodulation M of the base harmonic component of the measured fluorescence signal (80Mz). The intensity fraction f_i of each lifetime component may be found from the sine and cosine transforms of this signal.

$$S = \sum_i \frac{f_i \omega \tau_i}{1 + \omega^2 \tau_i^2} \tag{10}$$

$$G = \sum_i \frac{f_i \omega}{1 + \omega^2 \tau_i^2} \tag{11}$$

$$\sum_i f_i = 1 \tag{12}$$

$$Tan\phi = S/G \tag{13}$$

$$M = \sqrt{S^2 + G^2} \tag{14}$$

In the fitting routine, the lifetimes of the two forms are known from calibration measurements, hence the intensity fractions of the two components may easily be found[26]. To get the required concentration ratio it remains to normalize the intensity fractions f_1 and f_2 by the relative intensity of each form. In many cases, this can be assumed to be proportional to the lifetime ratio (1:1.4). In the case of BCECF, we found this not to be the case and normalized using the measured relative intensity ratio (1:5.9) of our calibration samples. The pH may then be calculated using equation (9).

Image slices were taken at increasing depth into the skin samples. The instrument was calibrated against a lifetime standard (Fluorescein, pH 9) to give corrected phase and modulation at each pixel in the image. A second calculation step, outlined above, gave the pH image. Some representative images are shown in figure 6.

The Intensity images generally show increased signal from the region of the cell walls and the structure of the sample is clearly visible in these image slices. At 8.5 microns into the sample, granulocytes with nuclei are visible. It is at this interface that we expect to see normal physiological pH. The pH images show the distribution of pH corresponding to the intensity images. There is a clear increase in pH in the deeper layers compared to the surface.

Histograms of the pH values for each slice were made and are shown in figure 7. The histograms show a double peaked structure, changing from a dominant peak at pH 6 to a peak at pH 7 as a transition is made from the stratum corneum to the stratum granulosum (indicated by the arrow). This data demonstrates the power of this technique to give three dimensional information about pH distribution previously unobtainable using tape stripping and a topically applied pH electrode.

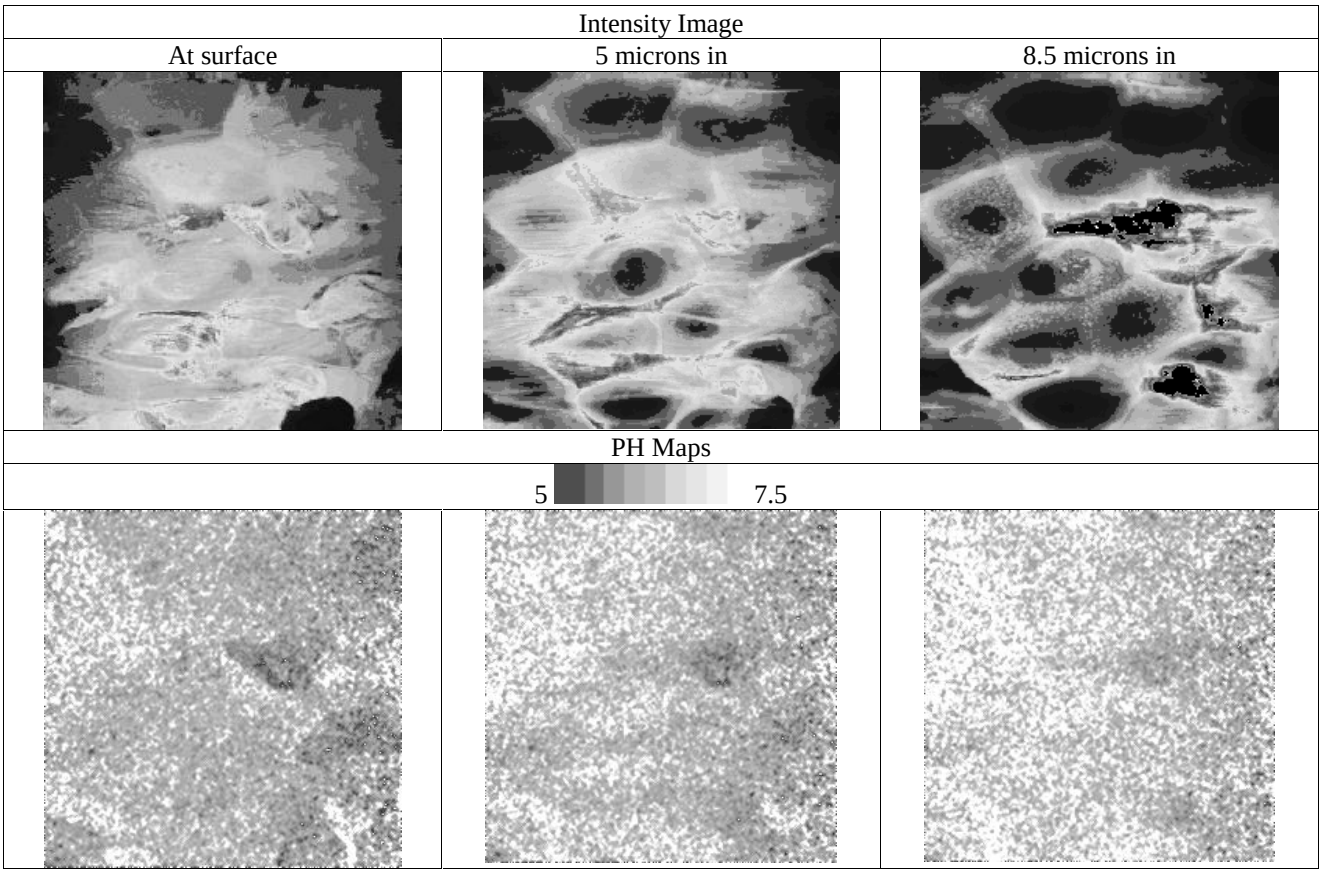

Figure 6. Intensity images of skin stained with BCECF and their corresponding pH maps as a function of depth.

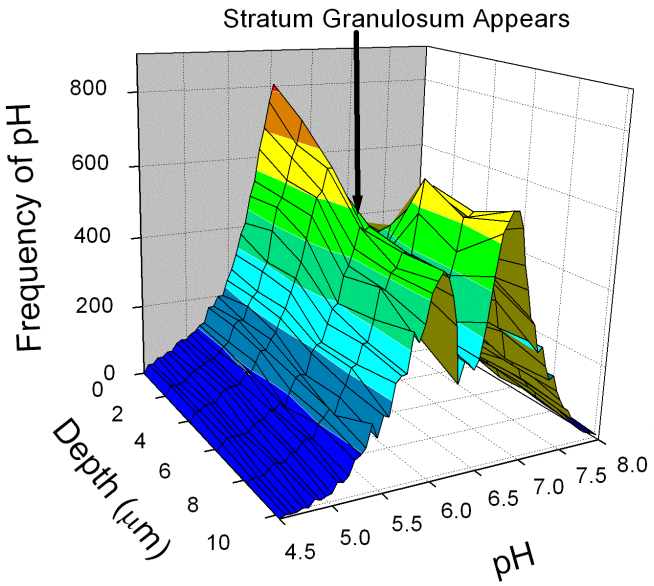

Figure 7. Histograms of the pH values for increasing depth into the skin. Frequency corresponds to the number of times a pixel is found with a particular pH value in an image slice.

4. Conclusions

We have described a frequency domain approach to the measurement of multiphoton excitation cross-sections and its implementation using a standard inverted microscope. This approach used the point spread function of a microscope objective to give a well characterized excitation volume. Under picosecond pulsed operation of the Ti sapphire laser, the pulse duration at the sample is free from significant temporal broadening (for the 10X objective), simplifying the system calibration. This technique allows the order of the excitation process (e.g. two or three excitation processes) to be distinguished. The intensity modulation approach also can give additional information about the slow time dynamics of the process. This offers a way to quantify photobleaching and the diffusion of free fluorophore into the excitation volume. The analysis of this aspect of the data is the subject of further development of this method. Measurement of the two-photon cross-section spectra for a number of commonly encountered fluorophores has been presented. This data was obtained using a standard quadratic fit.

A further application of ultrafast lasers to fluorescence lifetime imaging has been described. This approach has a number of advantages over standard wide field intensity imaging. The process produces sectioned images allowing 3D information to be deduced. Excitation in the near infrared also allows The use of lifetime has been shown to overcome difficulties associated with non uniform labeling when using fluorescent probes in tissue. The data obtained using a pH sensitive lifetime probe in skin samples has shown spatial information about the pH gradient in the Stratum Corneum that is not obtainable from the standard technique of tape stripping.

Acknowledgements

The Laboratory for Fluorescence Dynamics is supported by the NIH under NIH PHS P 41-RR03155.

References

1. W.Denk, J.H.Strickler, W.W.Webb, “Two-photon laser scanning microscopy” Science, **248,** pp73-76, 1990.
2. W.Denk, D.W.Piston, W.W.Webb, “Two photon molecular excitation in laser scanning microscopy” *Handbook of biological confocal microscopy*, Chapter 28 Plenum, NewYork, 1994.
3. D.L.Wokosin, V.E.Centoze, S.Crittenden,J.White, Bioimaging **4**, pp. 208-214. 1996
4. B.R.Masters, P.T.So, E.Gratton “Multiphoton excitation fluorescence microscopy and spectroscopy of in vivo human skin” Biophys. J. **72**, pp. 2405-2412, 1997.
5. M.Muller, J.Squire, G.J.Brakenhoff “Measurement of femtosecond pulses in the focal point of a high numerical aperture lens by two-photon absorption” Opp. Lett. **20**, pp. 1038-1040. 1995
6. M Goppert-Mayer. Ann.Phys. **9**, pp.273-295. 1931
7. J.P.Hermann, J.Ducuing “Absolute measurement of two photon cross section” Phys. Rev. A.**5**, pp.2557-2568, 1972.
8. J.P.Hermann, J.Ducuing “Dispersion of the two photon cross section in Rhodamine dyes” Op. Comms. **6**, pp. 101-105. 1972.
9. I.M. Catalano A. Cingolani “Absolute two photo fluorescence with low power cw lasers” Appl. Phys. Lett **38** pp. 745-747 1981.
10. R.D. Jones P.R.Callis “A power squared sensor for two photon spectroscopy and dispersion of second order coherence” J.Appl. Phys. **64** pp.4301-4305, 1988.
11. A Fischer, C Cremer, E.H.K Stelzer,“Fluorescence of coumarins and xanthenes after two photon absorption with a pulsed titanium sapphire laser” Applied Optics **34**, pp.1989-2003 1995.
12. C. Xu, J. Guild, W.W.Webb, W. Denk, “Determination of absolute two photon excitation cross sections by in situ second order autocorrelation” Op. Lett. **20**, pp. 2372-2374, 1995.
13. C Xu, W.W. Webb, “Measurement of two-photon excitation cross sections of molecular fluorophores with data from 690 to 1050 nm” J.Opt. Soc. Am. B., **13** pp. 481-491, 1996
14. R. Wolleschensky, T.Feurer, R. Sauerbrey, U.Simon “Characterisation and optimization of a laser scanning microscope in the femtosecond regime” Appl.Phys. B. **67**, pp 87-94, 1998.
15. J.B.Guild, C.Xu, W.W. Webb, “Measurement of group delay dispersion of high numerical aperture objective lenses using two photon excited fluorescence” Appl. Opt. **36**, pp 397-401, 1997.

16. H.Szmacinski, J.R.Lakowicz “Optical measurements of pH using fluorescence lifetimes and phase-modulation fluorimetry” Anal. Chem. **65**, pp.1668-1674, 1993
17. H. Lin, H.Szmacinski, J.R.Lakowicz “Lifetime based pH sensors: Indicators for acidic environments” Anal. Biochem. **269**, pp 162-167, 1999
18. H.Ohman, A.Vahlquist. “In vivo studies concerning a pH gradient in human stratum corneum and upper epidermis” Acta Derm. Venereol. (Stockh) **74**, 375-379, 1994S.
19. Dikstein, A.Zlotogorski “Measurement of skin pH” Acta Derm Venereol (Stockh) **185**, pp.18-20. 1994
20. H.Ohman, A.Vahlquist, “The pH gradient over the stratum corneum differs in x-linked recessive and autosomal dominant ichthyosis: a clue to the molecular origin of the acid skin mantle”. J. Investig. Derm. **111**, pp.674-677. 1998.
21. Mauro T, Holleran WM, Grayson S, Gao WN, Man M-Q, Kriehuber E, Behne M, Feingold KR, Elias PM. 1998. Barrier recovery is impeded at neutral pH, independent of ionic effects: implications for extracellular lipid processing. Arch. Dermatol. Res. (290):215-222.
22. RW Berg, MC Milligan, FC Sarbaugh. 1994. Association of skin wetness and pH with diaper dermatitis. Pediatr. Dermatol. 11:18-20.
23. P.T.C. So, T.French, WM.Yu, K.M. Berland , CY Dong, E. Gratton.. “Two-photon fluorescence microscopy: time-resolved and intensity imaging” In: *Fluorescence Imaging and Microscopy*. Herman B, Wang XF editors. New York: John Wiley and Sons. p 351-374. 1996
24. JR Alcala, E Gratton, DM Jameson. 1985. A multifrequency phase fluorometer using the harmonic content of a mode-locked laser. Anal. Instr. 14:225-250.
25. RP Haughland. 1998. Handbook of Fluorescent Probes and Research Chemicals. TZ Spence, editor. p 554
26. DM Jameson, E Gratton, RD Hall. 1984. The measurement and analysis of heterogenneous emissions by multifrequency phase and modulation fluorometery. Applied Spectroscopy Reviews 20:55-106.
27. K.M.Hanson, M.J.Behne, N.P.Barry, T.M.Mauro E.Gratton, R.M.Clegg, Submitted to Biophysical Journal